Applied Physics Letters ARTICLE scitation.org/journal/apl

Magnetic domain size tuning in asymmetric Pd/Co/W/Pd multilayers with perpendicular magnetic anisotropy

Cite as: Appl. Phys. Lett. **115**, 182408 (2019); doi: 10.1063/1.5123469
Submitted: 6 August 2019 · Accepted: 20 October 2019 ·
Published Online: 30 October 2019

D. A. Dugato,[1,2] J. Brandão,[2] R. L. Seeger,[1] F. Béron,[3] J. C. Cezar,[2] L. S. Dorneles,[1] and T. J. A. Mori[2,a)]

AFFILIATIONS

[1]Departamento de Física, Universidade Federal de Santa Maria (UFSM), 97105-900 Santa Maria RS, Brazil
[2]Laboratório Nacional de Luz Síncrotron (LNLS), Centro Nacional de Pesquisa em Energia e Materiais (CNPEM), 13083-970 Campinas SP, Brazil
[3]Instituto de Física Gleb Wataghin (IFGW), Universidade Estadual de Campinas (UNICAMP), 13083-859 Campinas SP, Brazil

[a)]**Electronic mail:** thiago.mori@lnls.br

ABSTRACT

Magnetic multilayers presenting perpendicular magnetic anisotropy (PMA) have great potential for technological applications. On the path to develop further magnetic devices, one can adjust the physical properties of multilayered thin films by modifying their interfaces, thus determining the magnetic domain type, chirality, and size. Here, we demonstrate the tailoring of the domain pattern by tuning the perpendicular anisotropy, the saturation magnetization, and the interfacial Dzyaloshinskii-Moriya interaction (iDMI) in Pd/Co/Pd multilayers with the insertion of an ultrathin tungsten layer at the top interface. The average domain size decreases around 60% when a 0.2 nm thick W layer is added to the Co/Pd interface. Magnetic force microscopy images and micromagnetic simulations were contrasted to elucidate the mechanisms that determine the domain textures and sizes. Our results indicate that both iDMI and PMA can be tuned by carefully changing the interfaces of originally symmetric multilayers, leading to magnetic domain patterns promising for high density magnetic memories.

The precise control of the nucleation processes of magnetic domain patterns is essential to achieve adequate functionality and performance for modern technologies. Much progress has been achieved recently as the stabilization of chiral structures such as skyrmions has been demonstrated either in nanostructures or in multilayer thin films presenting perpendicular magnetic anisotropy (PMA), even at room temperature and zero magnetic field.[1–4] Mainly being observed in systems with ferromagnetic/heavy metal (FM/HM) interfaces, which can easily be integrated in current technologies, these achievements have opened an avenue toward the use of PMA multilayers in future spintronics devices.[5] Indeed, PMA multilayers are a very fertile ground for studying magnetic interactions, since several physical properties of the FM/HM interface can be tuned in order to tailor the magnetic domain pattern. However, the role of these magnetic interactions in determining the domain's properties must be well understood before further magnetic device development.[6–8]

Magnetic anisotropy (K), saturation magnetization (M_s), and exchange stiffness (A_{ex}) determine the magnetic domain wall type (Néel or Bloch), chirality, and size. Their role in the magnetic configuration establishment in PMA multilayers has been studied for years.[9–14] More recently, the observation that magnetic skyrmions may be stabilized by Dzyaloshinskii-Moriya interaction (DMI), arising from broken inversion symmetry[15] and spin orbit coupling (SOC) in the case of FM/HM interfaces,[16] has given the DMI a major role in the study of domain wall patterns.[17,18]

In this sense, several combinations of FM and HM have been tried to fabricate asymmetric PMA multilayers (HM_A/FM/HM_B) searching for specific conditions to host chiral skyrmions preferably stabilized at room temperature and small magnetic fields.[12,16,19–21] On the other hand, small asymmetries introduced to originally symmetric multilayers have also been demonstrated to be a good strategy to tune the DMI in PMA multilayers.[22–24]

Here, we tune the magnetic properties of originally symmetric Pd/Co/Pd multilayers by inserting an ultrathin W layer in the system top interface (Pd/Co/W/Pd). The PMA presents a minimum when an ultrathin W layer is inserted. Using magnetic force microscopy (MFM) images acquired at the as-grown state, alongside with micromagnetic simulations, we show that the respective interfacial DMI

(iDMI) is around three times higher than that observed for thicker W layers or the reference symmetric Pd/Co/Pd. This strategy allows us to obtain a 60% decrease in the average domain size at room temperature, demonstrating an important route to tune magnetic multilayers for high density magnetic memory devices.

To study the magnetic domain pattern evolution with a varying asymmetry at the Co/Pd top interface, we grew multilayers based on a Pd(1 nm)/Co(0.5 nm)/W(t)/Pd(1 nm) structure, with a nominal thickness t = 0, 0.1, 0.2, 0.3, or 1.0 nm. The multilayers were deposited on silicon substrates by magnetron sputtering from metallic targets, at room temperature and 3 mTorr of argon atmosphere, and repeated 15 times [Fig. 1(a)].

Saturation magnetization and anisotropy field (H_k) were extracted from magnetic hysteresis curves measured in a LakeShore vibrating sample magnetometer (VSM), yielding the perpendicular anisotropy constant value, $K_{eff} = M_s H_k/2$.[10] Magnetic domain pattern images of the as-grown multilayers were acquired by magnetic force microscopy (MFM) with a NanoSurf Flex scanning probe microscope operating in the dynamic force mode. We used Multi75-G MFM (75 kHz) tips from Budget Sensors, which are coated by a cobalt alloy presenting magnetic moment and coercivity of roughly 10^{-16} Am^2 and 0.03 T, respectively. The images were acquired at room temperature and zero magnetic field, with the tip-surface distance about 60 nm. The magnetic domain homogeneity was confirmed through the observation of 5 images over distances of 1 mm between them. In addition, the experimental MFM images were compared with those obtained by micromagnetic simulations.

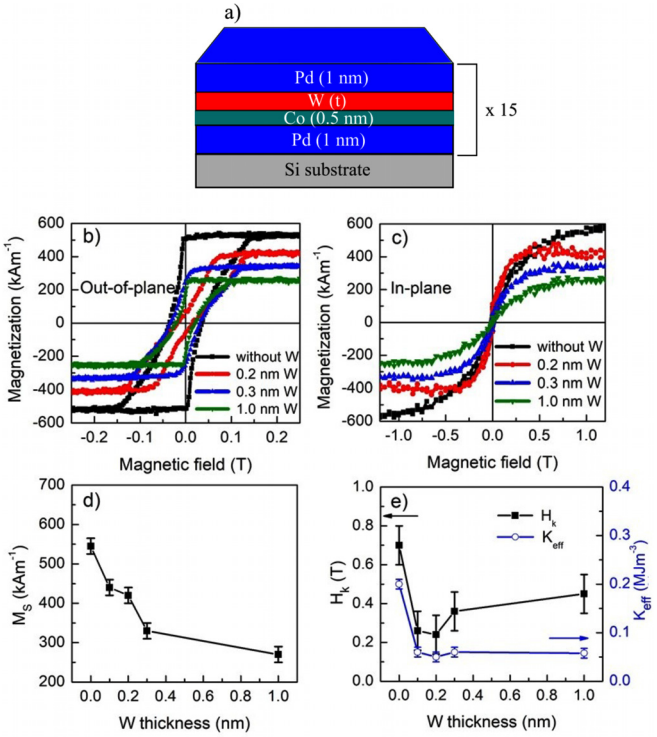

FIG. 1. Multilayer structure and magnetic properties. (a) Structure schematic. (b) and (c) Hysteresis loops recorded with the magnetic field applied along the out-of-plane and in-plane directions, respectively. (d) Saturation magnetization; (e) black squares: anisotropy field and open blue circles: anisotropy constant as a function of the W layer thickness.

For the modeling, we used the Mumax3 GPU-accelerated program to solve the time-dependent Landau-Lifshitz-Gilbert (LLG) equation to obtain the relaxation of the magnetization distribution.[25] The micromagnetic simulations were performed on an area of $5 \times 5\ \mu m^2$ discretized in cells of $3 \times 3 \times 7.5\ nm^3$ and using an effective medium approach to model the multilayer film as a single uniform layer.[26] The M_s and K_{eff} values extracted from the VSM measurements served as input, while we varied the iDMI contribution to understand its influence on the domain pattern formation without the applied magnetic field. Starting with a random initial magnetization, the equilibrium condition was obtained by minimizing the LLG energy terms with a relaxation time of 100 ns. The magnetic ground state represents the domain stability for each set of magnetic parameters. The energy of the effective iDMI was evaluated by comparing the simulated ground states with the corresponding MFM images using a methodology similar to what has been reported in the recent literature.[4,16,19,27,28]

Both out-of-plane and in-plane magnetic hysteresis loops indicate that all the multilayers present perpendicular magnetic anisotropy [Figs. 1(b) and 1(c)]. The extracted experimental values $M_s \sim 545$ kAm^{-1} and $K_{eff} \sim 0.2$ MJm^{-3}, observed for the reference sample, are in accordance with the values found in the literature for Pd/Co/Pd multilayers.[29] While the reference sample exhibits out-of-plane remanence very close to M_s, the remanence decreases for a very thin (0.1–0.2 nm thick) W layer and increases again, recovering a loop with nearly full remanence for the sample with a 1 nm W layer.

The W layer insertion leads to a saturation magnetization decrease, estimated by considering the entire Co volume [Fig. 1(d)]. The decline of the total magnetic moment may arise mainly from two coexisting mechanisms: (1) the formation of a magnetic dead layer due to alloying or interdiffusion at the interface[30] and (2) the reduction of magnetic proximity effect contribution to magnetization since, contrary to Pd, the spin and orbital magnetic moments of W may couple antiparallel to 3d metals.[31] Besides, both H_k and K_{eff} exhibit a minimum value for t = 0.2 nm [Fig. 1(e)] even though M_s decreases for thicker W layers. This PMA reduction with ultrathin W layer insertion can arise from an irregular Co/W-Pd interface, since such a thin layer should not percolate and can generate roughness instead. A rough Co/Pd interface is known to lessen the interface anisotropy and, consequently, the PMA.[32] At the same time, such a discontinuous W-Pd layer may lead to competing interfacial effects as Co/W and Co/Pd interfaces should behave differently. This scenario can also contribute to lower the PMA since the CoPd alloying, which is known to contribute to the strong anisotropy in Co/Pd multilayers,[33] is restricted by the coexistence of W along the interface.

Without the W layer, the MFM image shows a pattern of stripes and skyrmion-like circular domains that are normally observed in Co/Pd multilayers with thin Co thicknesses [Fig. 2(a)].[34,35] However, small labyrinth domains arise and the domain density increases significantly for t = 0.2 nm, reaching a magnetic domain periodicity (λ) of about 280 nm [Figs. 2(b) and 1(c)]. Hereafter, we define λ as the distance between two adjacent peaks in the magnetization profile and domain size as the full width at half maximum of a peak. While this system presents the lowest K_{eff} value along with an M_s average value, increasing to the 0.3 nm W layer yields a slightly larger K_{eff} combined to a M_s

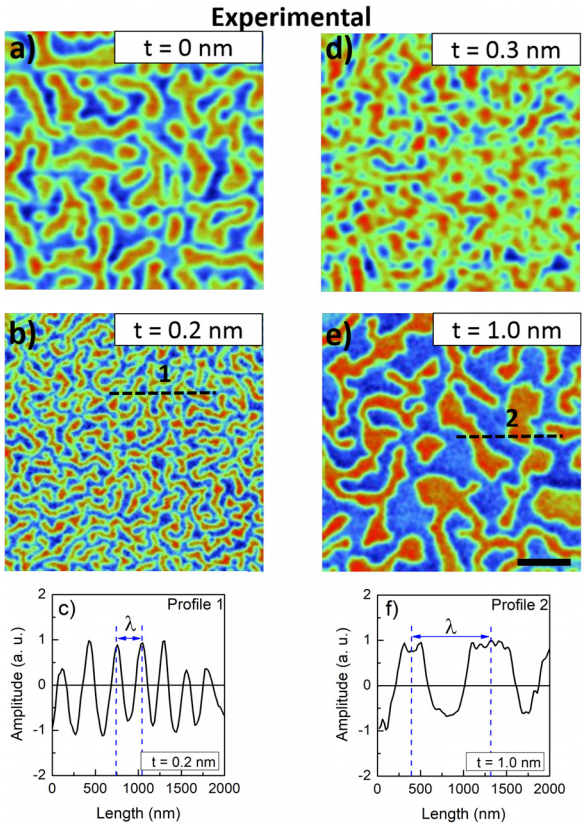

FIG. 2. Experimental magnetic force microscopy images acquired with zero magnetic field. (a), (b), (d), and (e) Pd/Co/Pd reference sample and multilayers with 0.2, 0.3, and 1.0 nm of W at the Co/Pd interface, respectively. (c) and (f) MFM profile measured along the straight lines highlighted on the MFM images in (b) and (e), respectively, where the periodicity λ is defined as the distance between two adjacent peaks. The scale bar in the images is 1 μm, and the color scale ranges from blue (amplitude −1, magnetization downward) to red (amplitude +1, magnetization upward).

decrease of around 25%, resulting in both the domain size and periodicity enlargement [Fig. 2(d)]. The domain size continues to increase for t = 1 nm, as the saturation magnetization continues decreasing [Figs. 2(e) and 2(f)]. In this case, the domain shape is similar to the reference sample, with a large periodicity of 670 nm and a domain density of ∼60% lower than with the 0.2 nm W layer.

In order to verify the role of the magnetic parameter in the magnetic domain pattern formation, we carried out micromagnetic simulations using the Mumax3 code. In a first attempt, we only used the experimental values extracted from the magnetization curves for K_{eff} and M_s, a fixed exchange stiffness $A = 12 \times 10^{-12}$ Jm^{-1}, and damping $\alpha = 0.3$. These preliminary simulated domain patterns exhibited distinct ground states compared to the ones observed in the measured MFM images, mainly for the samples with the ultrathin (0.1 and 0.2 nm) W layer. To reproduce the main features of the experimental images, a non-null interfacial Dzyaloshinskii-Moriya interaction—within 0.3 and 1.3 mJm^{-2}—had to be added to the simulated system.

Very good agreement with the experimental images is achieved with the additive iDMI, even for the nominally symmetric Pd/Co/Pd sample (Fig. 3). Although it should have a null iDMI in the ideal case, where the bottom and top interfaces contribute with the same amplitude but opposite sign, as represented in Fig. 4(a), the different qualities between the Pd/Co and Co/Pd interfaces may lead to small values of iDMI.[4,36,37] On the other hand, the combination of a bottom Pd/Co with a top Co/W interface is expected to yield a resulting negative iDMI [Fig. 4(b)]. This situation is similar to the iDMI reported for the Ru/Co/W system,[24] since both Co/Pd and Co/Ru interfaces present the same signal and similar amplitudes of iDMI.[38] Indeed, in the case of Ru/Co/W/Ru with varying W thicknesses, an iDMI peak has also been reported when the W thickness is about 0.2 nm.[24] In Ref. 24, the authors studied quasisymmetric multilayers with non-null iDMI focused on the isolated skyrmion nucleation and its behavior in the presence of an out-of-plane magnetic field. Here, we show that the interface engineering strategy of adding a "dusting" interlayer at the FM/HM interface can also be used to tune the magnetic domain size of worm-like patterns at zero magnetic field.

According to our micromagnetic simulations, the small iDMI observed for the symmetric sample rises about 3 times with the

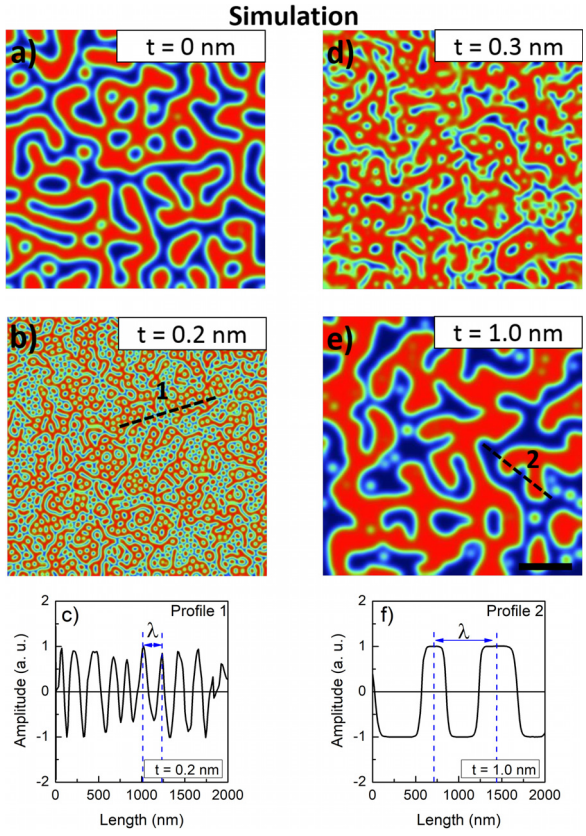

FIG. 3. Zero magnetic field micromagnetic simulated domain patterns with M_s and K_{eff} taken from VSM and non-null iDMI. (a), (b), (d), and (e) Pd/Co/Pd reference sample and multilayers with 0.2, 0.3, and 1.0 nm of W at the Co/Pd interface, respectively. (c) and (f) MFM profile measured along the straight lines highlighted on the MFM images in (b) and (e), respectively. The scale bar in the images is 1 μm, and the color scale ranges from blue (amplitude −1, magnetization downward) to red (amplitude +1, magnetization upward).

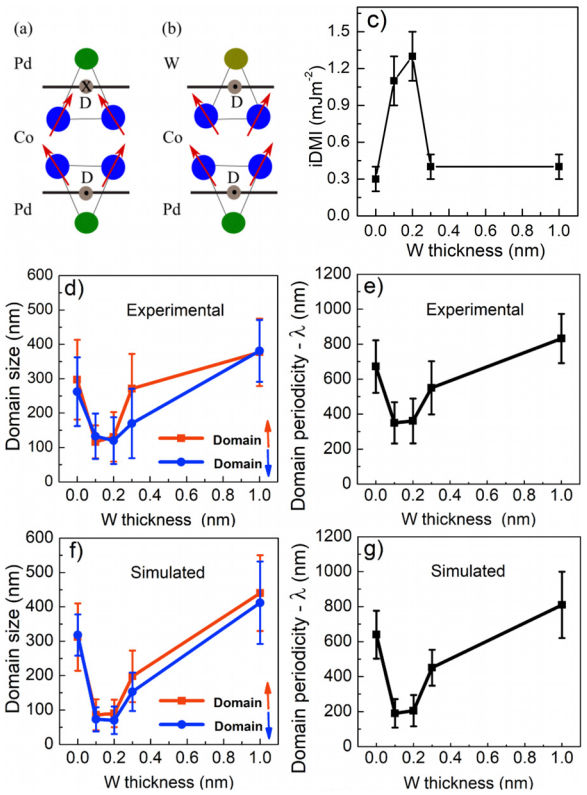

FIG. 4. Illustration of the resulting iDMI (D) in both (a) Pd/Co/Pd and (b) Pd/Co/W trilayers. (c) Dependence of the iDMI on the W thickness. (d) and (e) Domain size and periodicity, respectively, extracted from the experimental MFM images. For each sample, the values are averaged with a sampling of 25 line profiles (5 from each acquired image). (f) and (g) Domain size and periodicity, respectively, extracted from the simulated images. The domain size is estimated for both up and down domains.

insertion of an ultrathin layer of W (0.1–0.2 nm) at the top interface, as it is shown in Fig. 4(c). It is very interesting that a further minor increase in the W layer thickness (0.3 nm) leads to an iDMI almost as small as for the reference sample value. Note that this iDMI peak occurs for the same W thickness as the observed anisotropy minimum [see Fig. 1(e)]. The iDMI decline for thicker W layers is suggested to be due to the magnetic dead layer present when the W forms a continuous layer, which leads to the ferromagnetic layer degradation.[24,30] The thicker dead layer diminishes the orbital hybridization and consequently the SOC and magnetic exchange in both interfaces, which are important ingredients required for a strong iDMI.[39] Notwithstanding, the formation of very distinct domain patterns in the 0.1–0.2 nm range of W occurs due to atypically low K_{eff} values and an additive iDMI. Indeed, the geometric properties such as domain size and periodicity also present discrepant values in this range [Figs. 4(d) and 4(g)]. Similar to the results reported in Ref.30, here it is also likely that the small ratios between PMA and iDMI lead to smaller domain sizes as a result of the reduced energy of domain walls.[40]

In conclusion, we investigated the influence of a W layer, inserted at the top interface of a nominally symmetric Pd/Co/Pd multilayer, on the physical properties of the ferromagnetic Co layer as a function of its thickness. From hysteresis loops, we extracted the saturation magnetization M_s, anisotropy field H_k, and hence the perpendicular magnetic anisotropy K_{eff}. Both M_s and K_{eff} decay for thicker W layers. Most notably, a minimum of the anisotropy is observed with the insertion of an ultrathin 0.2 nm thick W layer.

MFM images were acquired to obtain the magnetic domain patterns at zero field and room temperature. Labyrinth domains were imaged, revealing a strong dependence of the size and periodicity on the W thickness. In particular, a domain size decrease of around 60% was obtained at 0.2 nm W, which coincides with the minimum perpendicular anisotropy, indicating that the physical properties of the multilayers play a direct role in the features of the magnetic domains.

To understand the magnetic domain formation, micromagnetic simulations were carried out and the results were compared with the experimental findings. By adjusting the physical parameters obtained for each W thickness in the modeling, the experimental observations were reproduced by taking into account the interfacial Dzyaloshinskii-Moriya interaction. The iDMI reaches a peak at 0.2 nm W and is remarkably reduced for thicker W layers. Very importantly, the small ratio between PMA and iDMI within the W thickness range 0.1–0.2 nm leads to very small domain sizes, which can be interesting for applications such as high density hard disk drives. The strategy of tuning magnetic domains by changing the interfaces of originally symmetric multilayers is promising on the path to develop devices based on skyrmions and chiral domain walls.

This study was financed in part by the Coordenação de Aperfeiçoamento de Pessoal de Nível Superior-Brasil (CAPES)-Finance Code 001, by the Fundação de Amparo à Pesquisa do Estado de São Paulo-São Paulo, Brasil (FAPESP)-Project No. 2012/51198-2, and by the Conselho Nacional de Desenvolvimento Científico e Tecnológico-Brasil (CNPq). J.C.C., L.S.D., and F.B. acknowledge grants provided by CNPq: Project Nos. 309354/2015-3, 302950/2017-6, and 436573/2018-0, respectively. F.B. acknowledges grant by FAPESP: No. 2017/10581-1. The samples were grown at the Microfabrication Laboratory-Brazilian Nanotechnology National Laboratory (LNNano). The micromagnetic simulations were carried out at the high performance computing facilities of the Brazilian Synchrotron Light Laboratory (LNLS) under Project No. 20180577.

REFERENCES

[1]A. Hrabec, J. Sampaio, M. Belmeguenai, I. Gross, R. Weil, S. M. Chérif, A. Stashkevich, V. Jacques, A. Thiaville, and S. Rohart, Nat. Commun. **8**, 15765 (2017).
[2]O. Boulle, J. Vogel, H. Yang, S. Pizzini, D. D. S. Chaves, A. Locatelli, T. O. Menteş, A. Sala, L. D. Buda-Prejbeanu, O. Klein, M. Belmeguenai, Y. Roussigné, A. Stashkevich, S. M. Chérif, L. Aballe, M. Foerster, M. Chshiev, S. Auffret, I. M. Miron, and G. Gaudin, Nat. Nanotechnol. **11**, 449–454 (2016).
[3]A. Fert, V. Cros, and J. Sampaio, Nat. Nanotechnol. **8**, 152–156 (2013).
[4]J. Brandão, D. A. Dugato, R. L. Seeger, J. C. Denardin, T. J. A. Mori, and J. C. Cezar, Sci. Rep. **9**, 4144 (2019).
[5]S. S. P. Parkin, M. Hayashi, and L. Thomas, Science **320**, 190–194 (2008).
[6]S. N. Piramanayagam, J. Appl. Phys. **102**, 011301 (2007).
[7]D. A. Allwood, G. Xiong, C. C. Faulkner, D. Atkinson, D. Petit, and R. P. Cowburn, Science **309**, 1688–1692 (2005).
[8]C. I. L. de Araujo, J. C. S. Gomes, D. Toscano, E. L. M. Paixão, P. Z. Coura, F. Sato, D. V. P. Massote, and S. A. Leonel, Appl. Phys. Lett. **114**, 212403 (2019).
[9]A. Barman, J. Appl. Phys. **101**, 09D102 (2007).

[10]B. Zhang, A. Cao, J. Qiao, M. Tang, K. Cao, X. Zhao, S. Eimer, Z. Si, N. Lei, Z. Wang, X. Lin, Z. Zhang, M. Wu, and W. Zhao, Appl. Phys. Lett. **110**, 012405 (2017).
[11]K. Shahbazi, A. Hrabec, S. Moretti, M. B. Ward, T. A. Moore, V. Jeudy, E. Martinez, and C. H. Marrows, Phys. Rev. B **98**, 214413 (2018).
[12]M. Belmeguenai, J.-P. Adam, Y. Roussigné, S. Eimer, T. Devolder, J.-V. Kim, S. M. Cherif, A. Stashkevich, and A. Thiaville, Phys. Rev. B **91**, 180405(R) (2015).
[13]S. Srivastava, K. Sivabalan, J. H. Kwon, K. Yamane, H. Yang, N. L. Chung, J. Ding, K. L. Teo, K. Lee, and H. Yang, Appl. Phys. Lett. **114**, 172405 (2019).
[14]G. Wei, X. Lin, Z. Si, N. Lei, Y. Chen, S. Eimer, and W. Zhao, Appl. Phys. Lett. **114**, 012407 (2019).
[15]S. Mühlbauer, B. Binz, F. Jonietz, C. Pfleiderer, A. Rosch, A. Neubauer, R. Georgii, and P. Böni, Science **323**, 915–919 (2009).
[16]C. Moreau-Luchaire, C. Moutas, N. Reyren, J. Sampaio, C. A. F. Vaz, N. V. Horne, K. Bouzehouane, K. Garcia, C. Deranlot, P. Warnicke, P. Wohlhüter, J.-M. George, M. Weigand, J. Raabe, V. Cros, and A. Fert, Nat. Nanotechnol. **11**, 444–448 (2016).
[17]I. Dzyaloshinsky, J. Phys. Chem. Sol. **4**, 241–255 (1958).
[18]T. Moriya, Phys. Rev. **120**, 91–98 (1960).
[19]A. Soumyanarayanan, M. Raju, A. L. G. Oyarce, A. K. C. Tan, M.-Y. Im, A. P. Petrović, P. Ho, K. H. Khoo, M. Tran, C. K. Gan, F. Ernult, and C. Panagopoulos, Nat. Mater. **16**, 898–904 (2017).
[20]J.-Y. Chauleau, W. Legrand, N. Reyren, D. Maccariello, S. Collin, H. Popescu, K. Bouzehouane, V. Cros, N. Jaouen, and A. Fert, Phys. Rev. Lett. **120**, 037202 (2019).
[21]H. L. T. Lin, S. Poellath, Y. Zhang, B. Ji, N. Lei, J. J. Yun, L. Xi, D. Z. Yang, T. Xing, Z. L. Wang, L. Sun, Y. Z. Wu, L. F. Yin, W. B. Wang, J. Shen, J. Zweck, C. H. Back, Y. G. Zhang, and W. S. Zhao, Phys. Rev. B **98**, 174425 (2018).
[22]R. Tolley, S. A. Montoya, and E. E. Fullerton, Phys. Rev. Mater. **2**, 044404 (2018).
[23]A. Hrabec, N. A. Porter, A. Wells, M. J. Benitez, G. Burnell, S. McVitie, D. McGrouther, T. A. Moore, and C. H. Marrows, Phys. Rev. B **90**, 020402 (2014).
[24]A. Samardak, A. Kolesnikov, M. Stebliy, L. Chebotkevich, A. Sadovnikov, S. Nikitov, A. Talapatra, J. Mohanty, and A. Ognev, Appl. Phys. Lett. **112**, 192406 (2018).
[25]A. Vansteenkiste, AIP Adv. **4**, 107133 (2014).
[26]S. Honda, Y. Ikegawa, and T. Kusuda, J. Magn. Magn. Mater. **111**, 273–292 (1992).
[27]A. V. Davydenko, A. G. Kozlov, A. G. Kolesnikov, M. E. Stebliy, G. S. Suslin, Y. E. Vekovshinin, A. V. Sadovnikov, and S. A. Nikitov, Phys. Rev. B **99**, 014433 (2019).
[28]S. Woo, K. Litzius, B. Kruger, M.-Y. Im, L. Caretta, K. Richter, M. Mann, A. Krone, R. M. Reeve, M. Weigand, P. Agrawal, I. Lemesh, M.-A. Mawass, P. Fischer, M. Klaui, and G. S. D. Beach, Nat. Mat. **15**, 501–507 (2016).
[29]B. Tudu, K. Tian, and A. Tiwari, Sensors **17**, 2743 (2017).
[30]A. G. Kolesnikov, A. V. Ognev, M. E. Stebliy, L. A. Chebotkevich, A. V. Gerasimenko, and A. S. Samardak, J. Magn. Magn. Mater. **454**, 78–84 (2018).
[31]F. Wilhelm, P. Poulopoulos, A. Scherz, H. Wende, K. Baberschke, M. Angelakeris, N. K. Flevaris, J. Goulon, and A. Rogalev, Phys. Status Solidi. A **196**, 33–36 (2003).
[32]C. W. Barton, T. J. A. Slater, R. M. Rowan-Robinson, S. J. Haigh, D. Atkinson, and T. Thomson, J. Appl. Phys. **116**, 203903 (2014).
[33]S.-K. Kima, V. A. Chernov, and Y.-M. Koo, J. Magn. Magn. Mater. **170**, L7–L12 (1997).
[34]H. Chihaya, M. Kamiko, and R. Yamamoto, J. Appl. Phys. **100**, 113707 (2016).
[35]W. Legrand, D. Maccariello, N. Reyren, K. Garcia, C. Moutafis, C. Moreau-Luchaire, S. Collin, K. Bouzehouane, V. Cros, and A. Fert, Nano Lett. **17**, 2703–2712 (2017).
[36]M. Quinsat, Y. Ootera, T. Shimada, M. Kado, S. Hashimoto, H. Morise, S. Nakamura, and T. Kondo, AIP Adv. **7**, 056318 (2017).
[37]A. W. J. Wells, P. M. Shepley, C. H. Marrows, and T. A. Moore, Phys. Rev. B **95**, 054428 (2017).
[38]Y.-K. Park, D.-Y. Kim, J.-S. Kim, Y.-S. Nam, M.-H. Park, H.-C. Choi, B.-C. Min, and S.-B. Choe, NPG Asia Mater. **10**, 995–1001 (2018).
[39]S. Kim, K. Ueda, G. Go, P.-H. Jang, K.-J. Lee, A. Belabbes, A. Manchon, M. Suzuki, Y. Kotani, T. Nakamura, K. Nakamura, T. Koyama, D. Chiba, K. T. Yamada, D.-H. Kim, T. Moriyama, K.-J. Kim, and T. Ono, Nat. Commun. **9**, 1648 (2018).
[40]A. Thiaville, S. Rohart, É. Jué, V. Cros, and A. Fert, Europhys. Lett. **100**, 57002 (2012).